ACADEMIA ROMÂNĂ
Revue Roumaine de Chimie
http://web.icf.ro/rrch/

Rev. Roum. Chim.,
2014, *59*(6-7), 575-583

Dedicated to the memory of
Professor Eugen Segal (1933-2013)

HYDROGEN-BONDED SUPRAMOLECULAR STRUCTURE BUILT ON THE BASIS OF FERROCENECARBOXYLIC ACID AND 4,4'-AZOPYRIDINE

Angelica VLAD,[a] Mirela-Fernanda ZALTARIOV,[a] Maria CAZACU,[a,*] Loredana VACAREANU,[a] Sergiu SHOVA[b] and Constantin TURTA[b]

[a] "Petru Poni" Institute of Macromolecular Chemistry, Aleea Gr. Ghica Voda 41A, 700487 Iaşi, Roumania
[b] Institute of Chemistry of ASM, Academiei str. 3, Chisinau 2028, Republic of Moldova

Received April 30, 2014

A ferrocene supramolecular structure, **1**, has been generated by mixing ferrocenecarboxylic acid with 4,4'-azopyridine in methanol, in the presence of 2,6-lutidine as a base. Both FTIR spectrum and single crystal X-ray diffraction revealed association through hydrogen bonds were carboxylic group acts as donor while pyridine nitrogen as acceptor. The spin state of the iron atom was verified by Moessbauer spectroscopy while the redox behavior was studied by cyclic voltammetry.

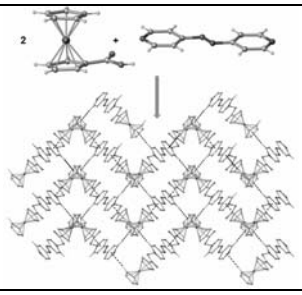

INTRODUCTION

Compounds which are able to self-assemble in functional supramolecules and/or to suffer reversible structural transformations as responses to environmental changes are of interest for applications in advanced sensors. Their nanostructuration patern, as well as physical or chemical properties can be changed as a response to external stimuli such as pH, electron-transfer, light, temperature, etc.[1,2] Between them, the redox stimulus is of high interest because it can effectively influence or induce a series of changes of physicochemical property in a molecular system which contains a suitable center. The redox state changes of one of the components can lead to structural modification of the whole assembly.[2] This allows the development of responsive materials controlled by electrochemical reversible complexes.[1] Many electrochemical responsive supramolecular systems have been achieved in solid state, in diluted solutions (including micelles or vesicles) or as polymeric hydrogels.[1]

The achievements so far in supramolecular chemistry strongly promote the development of ferrocene-associated electrochemical responsive materials.[1] Ferrocene (Fc) and its derivatives, due to their redox characteristics, can be chosen as redox-switchable groups for supramolecular complexes. The conversion of ferrocene unit, from its hydrophobic nonpolar neutral state, Fe(II), to the hydrophilic ferrocenium cation, can lead to changes in the amphiphilicity of supramolecular complexes and, as a result, their behavior and structuration in a lyotropic medium.[2] Ferrocene in its reduced state, as a neutral compound, forms inclusion complexes, with cyclodextrine; when ferrocene is in oxidized state (Fc^+), as a cation, the

* Corresponding author: mcazacu@icmpp.ro

complexes formed are very weak.[1] Ferrocene–cyclodextrin conjugates were investigated, as potential synthetic enzymes or redox-switching systems.[3] On the other hand, ferrocene based ligands, due to conformational flexibility of the ferrocenyl rings, are of interest for building novel structural motifs.[4] It has been found that ferrocenecarboxylic acid forms a 1:2 adduct in salt form with hexamethylenetetramine.[5] Carboxylic groups, which are able to involve in two hydrogen bonds, are suitable for creation of supramolecular structures. Thus, ferrocenecarboxylic acid (FcCOOH) itself forms two-dimensional quasicrystallites with orders to long distance.[6]

A supramolecular architecture based on ferrocenecarboxylic acid and 4,4'-azopyridine is reported here. Due to its special structure (larger π-bond conjugated system and two active nitrogen atoms), 4,4'-azopyridine is especially suitable as building block for supramolecular systems with or without metal.[7] The structure of the assembly was revealed by X-ray single crystal diffraction while the iron spin state was determined by Moessbauer spectroscopy. The redox behavior of the complex was studied by cyclic voltammetry.

RESULTS AND DISCUSSION

Ferrocenecarboxylic acid was treated with 4,4'-azopyridine in 2:1 molar ratio in methanol, in a basic medium created by adding 2,6-lutidine aiming to obtain a supramolecular structure, **1** (Scheme 1). The needle brown crystals grown in a few days proved indeed to be a supramolecular structure built by hydrogen bonding of the two components in the designed molar ratio (FcCOOH: AzPy=2:1).

The formation of the hydogen bonds is well emphasized by the presence of broad absorption bands at 2473 and 1859 cm^{-1} in IR spectrum (Fig. 1a).[8] The bands at 1585 cm^{-1} (pyridyl ring) and 1653 cm^{-1} (Fc-COOH) in the spectra of the two components are shifted to 1593 cm^{-1} and 1688 cm^{-1}, respectively in the spectrum of the supramolecular structure. The band at 1564 cm^{-1} attributed to aromatic C=C in azopyridine rings is shifted with 4 cm^{-1} to higher wavenumber (Fig. 1a). The band at 1408 cm^{-1} in the FTIR spectrum of the supramolecular structure is attributed to the stretching vibration of N=N group, shifted with 6 cm^{-1} at lower waveumber as compared with 4,4'-azopyridine.[9] In addition, large and intense bands can be seen on the spectrum of the compound 1 at 1859 and 2473 cm^{-1} assigned to the hydrogen bonds.

The result of X-ray single crystal study is depicted in Fig. 2, whole bond lengths and angles are summarized in Table 1. It has been demonstrated compound **1** to crystalize in monoclinic system $P2_1/c$ space group. Its crystal is built as the result of co-crystallisation of feorrocenecarboxylic acid and 4,4′-azopyridine in 2:1 ratio. The main structural unit represents a centrosymmetric associate about the mid-point of the N=N bond stabilized *via* strong intermolecular O-H···N hydrogen bonding, where carboxylic group acts as donor and pyridine nitrogen as acceptor: O−H···N [O−H 0.82 Å, H···N 1.89 Å, O1···N 2.679(3) Å, O1−H···N1 179.8°]. The cyclopentadienyl rings of the ferrocene moiety are eclipsed with the bond lengths and angles in the normal ranges for the ferrocene compounds.

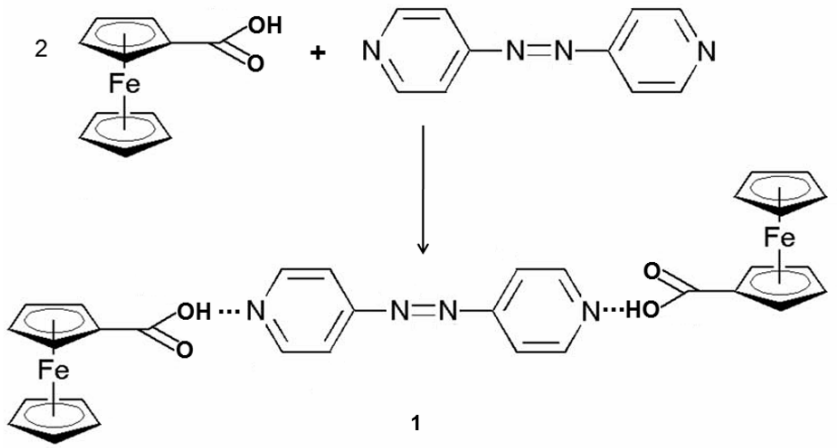

Scheme 1 – The reaction path for obtaining ferrocene-supramolecular structure, **1**.

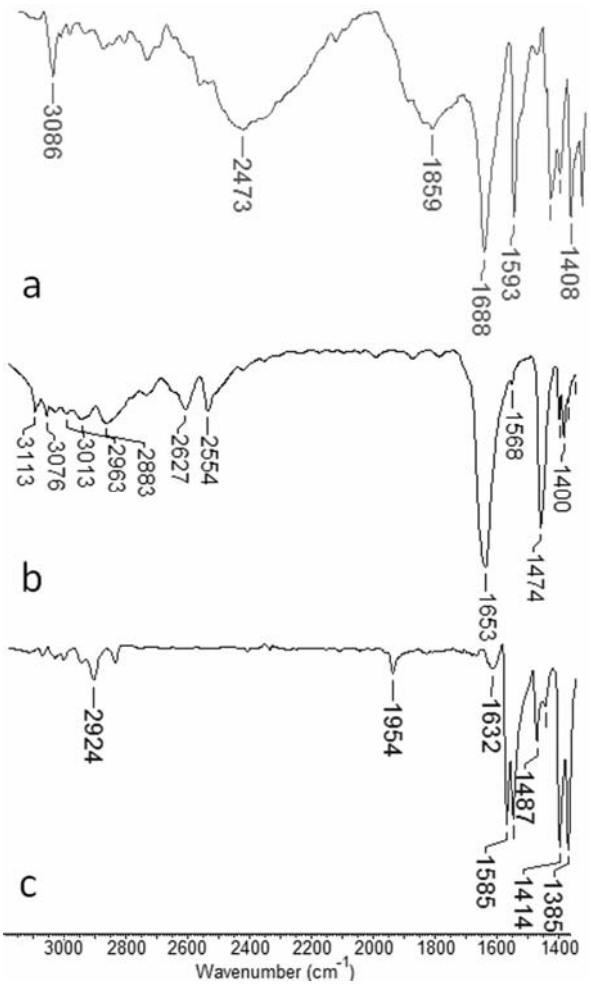

Fig. 1 – FTIR spectra for: a- ferrocene-supramolecular structure **1;** b - ferrocenecarboxylic acid; c – 4,4'-azopyridine in the region 1400-3200 cm^{-1}.

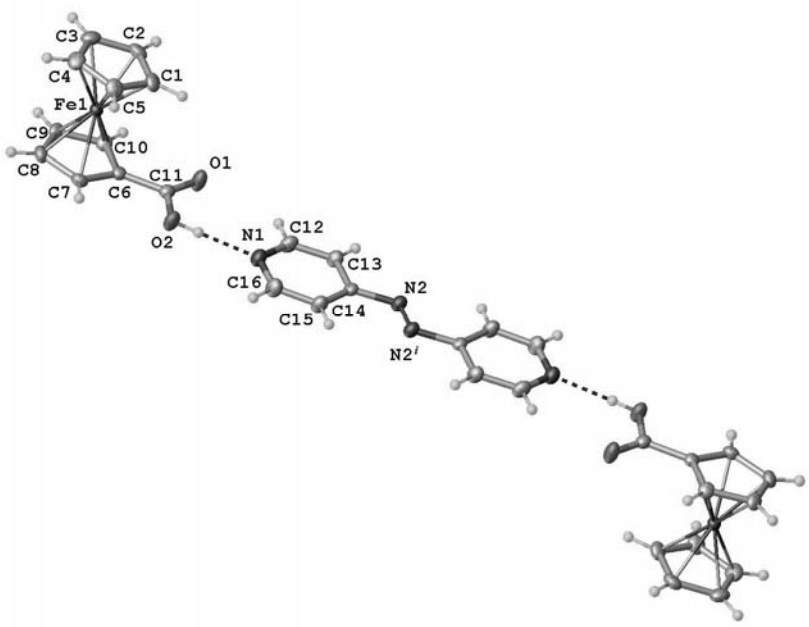

Fig. 2 – X-ray structure of compound **1**. Atomic displacement parameters are drawn at 50% probability level. Symmetry code: $^{i)}$ 1 – *x*, 1 - *y*, 2 – *z*.

Table 1

Selected bond lengths (Å) and bond angles (°) for **1**

Fe1-C10	2.032(2)	C7-C8	1.415(3)
Fe1-C6	2.026(2)	C5-C4	1.410(3)
Fe1-C7	2.036(2)	C5-C1	1.423(3)
Fe1-C5	2.032(2)	C9-C8	1.419(3)
Fe1-C9	2.050(2)	C2-C3	1.415(3)
Fe1-C8	2.048(2)	C2-C1	1.412(3)
Fe1-C2	2.028(2)	C4-C3	1.413(3)
Fe1-C4	2.049(2)	N1-C12	1.329(3)
Fe1-C3	2.048(2)	N1-C16	1.342(3)
Fe1-C1	2.025(2)	C13-C14	1.387(3)
O1-C11	1.212(2)	C13-C12	1.374(3)
O2-C11	1.319(2)	C14-C15	1.389(3)
C10-C6	1.423(3)	C14-N2	1.426(3)
C10-C9	1.412(3)	C16-C15	1.370(3)
C11-C6	1.471(3)	N2-N2[1]	1.247(3)
C6-C7	1.426(3)		
C9-C10-C6	108.2(2)	C4-C3-C2	108.0(2)
O-C11-O21	123.6(2)	C2-C1-C5	107.8(2)
O1-C11-C6	123.0(2)	C12N1-C16	117.3(2)
O2-C11-C6	113.4(2)	C12-C13-C14	118.8(2)
C10-C6-C11	124.1(2)	C13-C14-C15	118.5(2)
C10-C6-C7	107.5(2)	C13-C14-N2	116.3(2)
C8-C7-C6	108.1(2)	C15-C14-N2	125.2(2)
C4-C5-C1	107.9(2)	N1-C12-C13	123.4(2)
C10-C9-C8	108.3(2)	N1-C16-C15	123.7(2)
C7-C8-C9	108.0(2)	C16-C15-C14	118.3(2)
C1-C2-C3	108.1(2)	N2[1]-N2-C14	113.4(2)
C5-C4-C3	108.2(2)		

Symmetry code: [i] 1 – *x*, 1 - *y*, 2 – *z*.

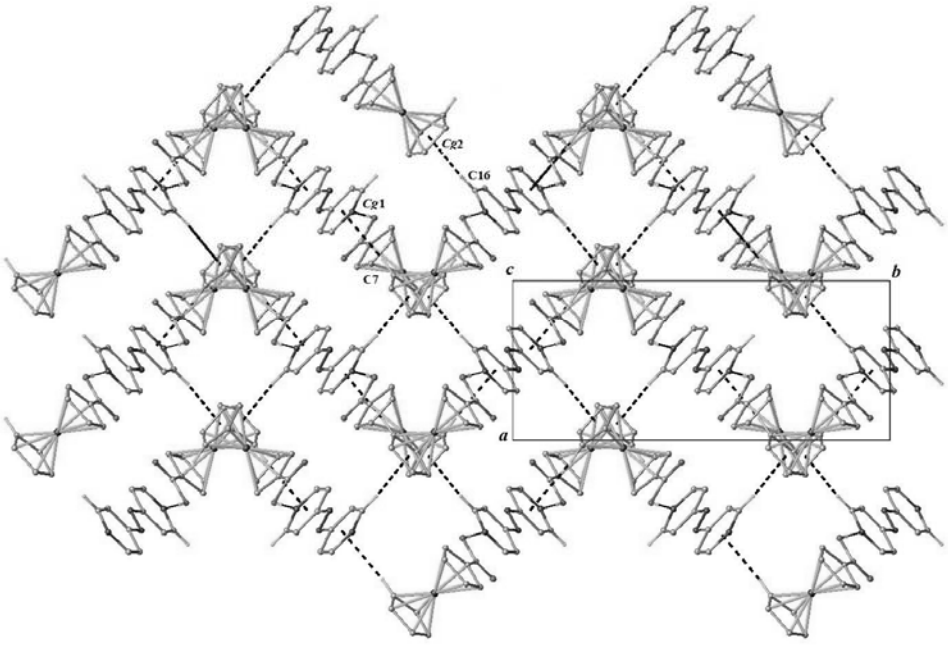

Fig. 3 – View of packing diagram along *c* crystallographic axis.

C-H···π stacking parameters:

C16−H···*Cg*2 [C16−H 0.93 Å, H···*Cg*2 2.87 Å, C16···*Cg*2 3.68(3) Å, C16−H···*Cg*2 147.0°]; C7−H···*Cg*1 [C7−H 0.93 Å, H···*Cg*1 2.86 Å, C7···*Cg*1 3.75(3) Å, C7−H···*Cg*1 161.2°] *Cg*1 and *Cg*2 are the centroids of N1/C12/C13/C14/C15/C16 and C1/C2/C3/C4/C5 rings, respectively.

The packing of the above mentioned associates in the crystal results into the formation of a tree-dimensional supramolecular network mediated *via* C-H···π stacking interactions, as shown in Fig. 3.

Mossbauer spectra of the sample show a very intensive doublet (Fig. 4) both at 80 K and room temperature with the parameters given in Table 2. By comparing values of isomer shift (IS, δ_{Fe}) and quadrupole splitting (QS) with literature data, one can see that they are practically the same (in error limits) as for FcCOOH.[10] Temperature dependence of IS value of the sample is well explicable within the limits of the second-order Doppler effect.[11] The formation of hydrogen bonds between FcCOOH and AzPy does not change the electron charge density around the nucleus ^{57}Fe. There is no observed change in temperature dependence of the electric field gradient (EFG) around the iron nucleus in the studied sample in comparison with FcCOOH. One of the most obvious explanations would be the increased of the lattice contribution (q_{Lat}) in EFG value for pure FcCOOH relative to studied compound **1**.

The electrochemical behavior was investigated by recording the cyclic voltammograms of the ferrocene-supramolecular structure in DMF solution containing tetrabutylammonium tetrafluoroborate ($TBABF_4$) as supporting electrolyte. The current-potential curves were recorded by sweeping the working electrode potential on both negative and positive potential range, at a constant scan rate of 50 mV s^{-1}. Multi-cyclic voltammograms were also recorded in the positive and negative range of potential. The voltammograms were compared with those of the electrolyte and ferrocenecarboxylic acid. The electrochemical data of the analysis are summarized in Table 3.

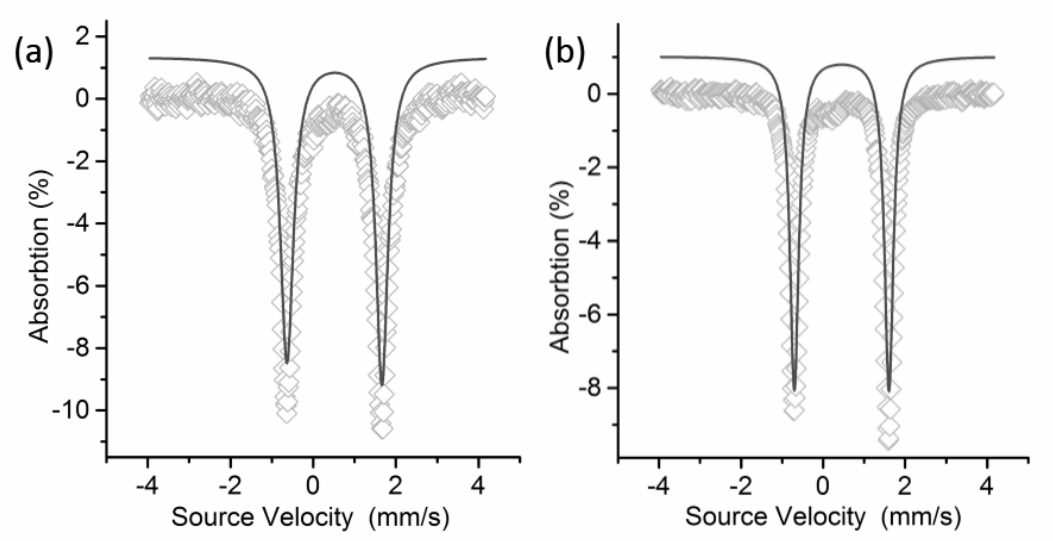

Fig. 4 – The Mossbauer spectra of **1** at: a) - 80 K and b) - 300 K.

Table 2

Mössbauer data for the ferrocene-containing supramolecular structure

Sample	T, K	mm/s				
		Isomer shift, IS[a] (error=±0.020)	**Quadrupole splitting, QS (error=±0.020)**	**Width**	**Relative surface**	**Ref.**
1	300	0.449	2.278	0.258	1.000	experimental
FcCOOH		0.440	2.164	-	-	[11]
1	80	0.513	2.269	0.380; 0.355	1.044	experimental
FcCOOH		0.480	2.340	-	-	[11]

[a]Isomer shift is presented relative to Fe metal.

Table 3

The main data from cyclic votammograms

	E_{pa} (V)			E_{pc} (V)			ΔE_a(V)			$E^{o'}$(V)		
	E_{pa1}		E_{pa2}	E_{pc1}	E_{pc2}	E_{pc3}						
TBATFB	-		-		-		-			-		
FcCOOH	0.824		-	0.705	0.453	0.320	0.119			0.764		
	E_{pa1}'		E_{pa2}'		E_{pc1}'		$\Delta E_a'$			$E^{o'}$		
	-0.874		-		-0.953		0.079			-0.893		
1	0.784		1.337	0.690	1.159	0.068	0.094		0.178	0.737		1.248
	E_{pa1}'	E_{pa2}'	E_{pa3}'	E_{pc1}'	E_{pc2}'	E_{pc3}'	$\Delta E_1'$	$\Delta E_2'$	$\Delta E_3'$	$E^{o'1'}$	$E^{o'2'}$	$E^{o'3'}$
	-0.474	-0.605	-1.283	-0.553	-0.763	-1.509	0.079	0.158	0.226	-0.513	-0.684	-1.396

E_{pa1}-anodic potential of the first peak in positive range of potential; E_{pa2}-anodic potential of the second peak in positive range of potential; E_{pc1}-cathodic potential of the first peak in positive range of potential; E_{pc2}-cathodic potential of the second peak in positive range of potential; E_{pc3}-cathodic potential of the third peak in positive range of potential; E_{pa1}'-anodic potential of the first peak in negative range of potential; E_{pa2}'-anodic potential of the second peak in negative range of potential; E_{pa3}'-anodic potential of the third peak in negative range of potential; E_{pc1}'-cathodic potential of the first peak in negative range of potential; E_{pc2}'-cathodic potential of the second peak in negative range of potential; E_{pc3}'-cathodic potential of the third peak in negative range of potential; ΔE-the peak potential difference ($\Delta E = E_{pa} - E_{pc}$); E_o'-the formal redox potential ($E_o' = (E_{pa}+E_{pc})/2$).

In Fig. 5 are shown the cyclic voltammograms recorded for the analyzed compounds, by sweeping the working electrode potential in the positive range of potential. It can be seen that the cyclic voltammograms of the supramolecular structure exhibit two quasi-reversible redox couple with oxidation/reduction peaks potentials located at 0.784 V/ 0.690 V and 1.337 V/ 1.159 V, having peak to peak separation (ΔEp) at about 0.094 V and 0.178 V. The first redox couple can be assigned to the one-electron oxidation/reduction processes of the ferrocene (Fc) and ferrocenium cation (Fc^+) redox centers[12]. The formal potential of the ferrocene carboxylic acid ($E^{o'}$ = 0.764 V) seems to be slightly higher than in the case of ferrocene ($E^{o'}$ = 0.550 V *vs* Ag/AgCl, measured at the beginning of the experiments), and this can be due to the electron-withdrawing properties of the carboxylic group. The azo (-N=N-) group is highly susceptible to the reduction process and thus, it can undergo a cathodic reduction process followed by protonation reaction. The cyclic voltammograms recorded for ferrocene-supramolecular structure at different scan rates show a linear relationship between the anodic current peak values and the scan rates. The redox current peaks values increased as the scan rates values are increased from 20 to 200 mVs^{-1}, and this suggests that the redox processes are quasi-reversible and governed by diffusion transport processes (Fig.5 (d)). Furthermore, with a continuous cyclic scan for 10 cycling on the same positive potential range, with 50 mVs^{-1}, the voltammetric response shows a gradual decrease in peak currents intensities as the number of the scans are increased, indicating the consumption of the electroactive species at the electrode surface-solution interface as the oxidation/reduction processes of the ferrocene complex occurred. At the end of the multiple scans no visible deposition was observed on the working electrode surface (Fig. 5 (c)). On the negative potential range (Fig. 6) the supramolecular structure exhibits three well defined and reversible redox peaks assigned to three reversible (consecutive) oxidation/reduction processes. By comparing the voltammograms of the ferrocene carboxylic acid and supramolecular structure, it can be seen that the latter exhibits new reversible redox couple peaks, assignable to the oxidation/reduction of the supramolecular structure. The effect of scan rate on the redox peaks for the supramolecular structure was studied in the range from 20 to 200 mV/s. The current intensities of the anodic peaks are increased while for cathodic peaks are decreased as the scan rate is increasing, and the values are shifted to more positive (E_{pa}) and negative (E_{pc}), respectively. The plot of redox peaks current values versus the scan rate values is almost linear which indicate that the ferrocene-supramolecular structure undergo reversible redox processes in the negative range. By running multi-cyclic voltammograms, it can be seen that by increasing the number of cycles the current intensities of the anodic and catodic peaks is diminished.

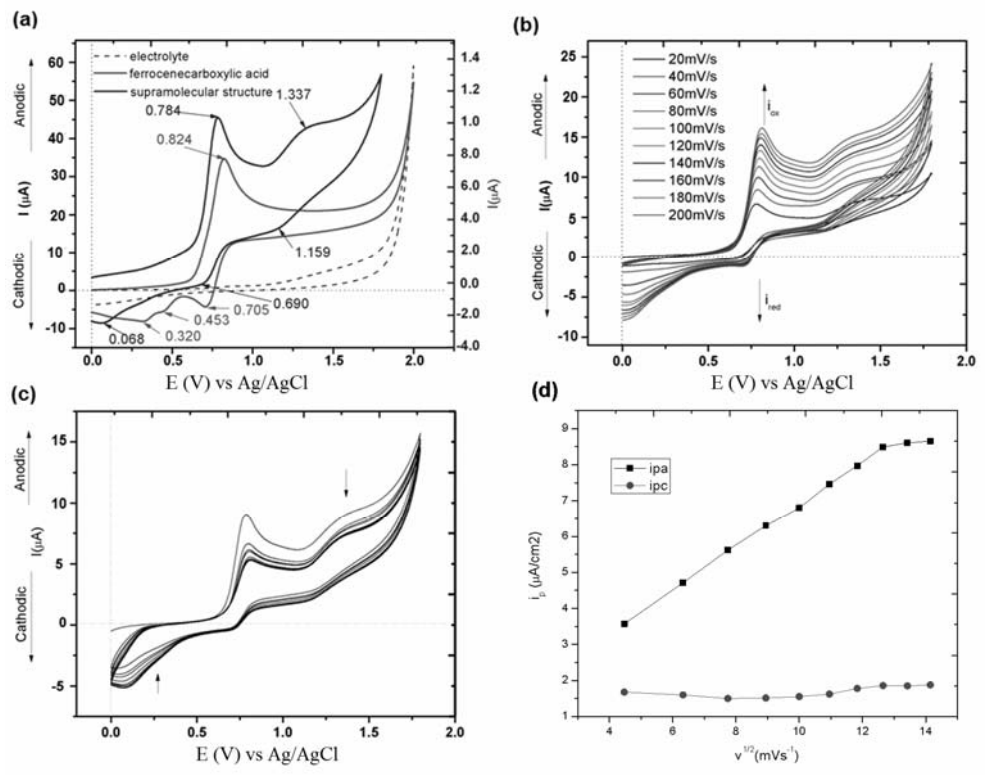

Fig. 5 – (a) Cyclic voltammogram recorded during the potential electrode scanning from 0.0 to 1.8 V range with 50 mV/s scan rate; (b) Cyclic voltammograms of the compound 1 recorded at different scan rates (from 20 to 200 mV/s); (c) the multi-cyclic voltammograms recorded for the ferrocene-supramolecular structure on the positive range of potential, at 50 mVs^{-1}; (d) the plot of the square-root of the scan rate ($v^{1/2}$) versus peak current (i_{pa} and i_{pc}).

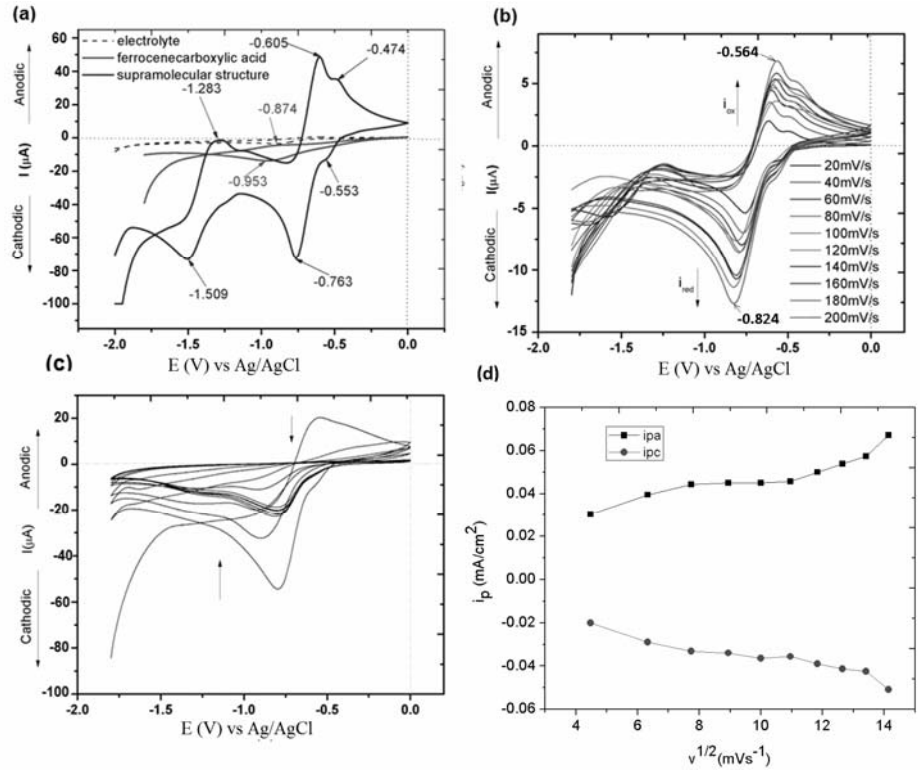

Fig. 6 – (a)Cyclic voltammogram recorded during the potential electrode scanning from -1.8 V to 0.0 V, with 50 mV/s scan rate; (b) cyclic voltammograms of the compound 1 recorded at different scan rates (from 20 to 200 mV/s); (c) the multi-cyclic voltammograms recorded on the negative range of potential, with 50 mVs^{-1} scan rate; (d) the plot of the square-root of the scan rate ($v^{1/2}$) versus peak current (i_{pa}) (E_{pa1}= -0.605 V) and (i_{pc}) (E_{pc2} = -0.763 V).

EXPERIMENTAL

Materials

Ferrocenecarboxylic acid (FcCOOH), 4,4'-azopyridine (AzPy), tetrabutylammonium tetrafluoroborate (TBATFB), and 2,6-dimethylpyridine were purchased from Sigma Aldrich, while the solvents (chloroform, tetrahydrofuran, methanol, ethanol and acetonitrile) were acquired from Chimopar S.A. and were used as received.

Ecquipments

Fourier transform infrared (FT-IR) spectra were recorded using a Bruker Vertex 70 FT-IR spectrometer. Analyses were performed in the transmission mode in the range 400-4000 cm^{-1} at room temperature with a resolution of 2 cm^{-1} and accumulation of 32 scans. The samples were incorporated in dry KBr and processed as pellets in order to be analyzed.

The Mössbauer spectra were acquired using a conventional spectrometer in the constant-acceleration mode (MS4, Edina,USA) equipped with a ^{57}Co source (~1.0 GBq) in a rhodium matrix. Isomer shifts are given relative to α-Fe at room temperature. The sample was measured at room temperature (RT) and 80 K and the spectra were fitted using the VMOS Fitting Program.

The Cyclic voltammograms were recorded using a Bioanalytical System, Potentiostat-Galvanostat (BAS 100B/W). All the experiments were performed in a one-compartment cell using a standard three-electrode cell arrangement with a working platinum electrode (disk shape, Φ= 1.6 mm), an auxiliary electrode (platinum wire), and a reference electrode (consisted of a silver wire coated with AgCl). Before each experiment, the Pt working electrode was cleaned by polishing it successively with 0.3 and 0.05 μm Al_2O_3 slurry on emery paper to a mirror finish, and then washed with methanol and bidistillated water. The electrochemical studies were carried out in DMF solution and containing tetrabutylammonium tetrafluoroborate ($TBABF_4$) as supporting electrolyte. Prior to each experiment, the monomer and polymer solutions were deoxygenated by passing dry argon gas for 10 min, and all measurements were performed at room temperature (25 ºC). The oxido-reduction potentials values are reported with respect to Ag/AgCl, which was previously calibrated using ferrocene (Fc) as an external reference ($E^{1/2}_{Fc/Fc+}$ = + 0.521 V *vs* Ag/AgCl).

X-ray Crystallography

X-ray diffraction data were collected with an Oxford-Diffraction XCALIBUR E CCD diffractometer equipped with graphite-monochromated Mo*K*α radiation. The single crystal was positioned at 40 mm from detector and 193 frames were measured each for 5 s over 1° scan width. The unit cell determination and data integration were carried out using the CrysAlis package of Oxford Diffraction.[13] The structure was solved by direct methods using Olex2[14] software with the SHELXS structure solution program and refined by full-matrix least-squares on F² with SHELXL-97.[15] Atomic displacements parameters for non-hydrogen atoms were refined using an anisotropic model. All H atoms attached to carbon were placed in fixed, idealized positions and refined as rigidly bonded to the corresponding non-hydrogen atoms. Positional parameters for hydrogen atom attached to O was obtained from difference Fourier synthases and verified by corresponding H-bond parameters. The molecular plots were obtained using the Olex2 program. Table 4 provides a summary of the crystallographic data together with refinement details. CCDC-1000007 contains the supplementary crystallographic data for this contribution. These data can be obtained free of charge from the Cambridge Crystallographic Data Centre via www.ccdc.cam.ac.uk/data_request/cif.

Table 4

Crystallographic data, details of data collection and structure refinement

Empirical formula	$C_{16}H_{14}FeN_2O_2$ (**1**)
formula weight	322.14
temperature/K	200
crystal system	monoclinic
space group	$P2_1/c$
a/Å	7.4186(3)
b/Å	16.6048(5)
c/Å	11.5466(5)
α/°	90.00
β/°	108.104(4)
γ/°	90.00
V/Å^3	1351.94(9)
Z	4
D_{calc}/mg/mm^3	1.583
μ/mm^{-1}	1.120
crystal size/mm^3	0.15 × 0.15 × 0.10
$\theta_{min,}$ θ_{max}(°)	4.9 to 49
reflections collected	6001
independent reflections	2118[R_{int} = 0.0303]
data/restraints/parameters	2118/0/191
R_1[a](I>2σ(I))	0.0266
wR_2[b](all data)	0.0646
GOF[c]	1.049
largest diff. peak/hole/e Å^{-3}	0.22/-0.28

[a] $R_1 = \Sigma||F_o| - |F_c||/\Sigma|F_o|$, [b] $wR_2 = \{\Sigma[w\,(F_o^2 - F_c^2)^2]/\Sigma[w(F_o^2)^2]\}^{1/2}$.
[c] GOF = $\{\Sigma[w(F_o^2 - F_c^2)^2]/(n-p)\}^{1/2}$, where n is the number of reflections and p is the total number of parameters refined.

Procedure

FcCOOH (0.1 g, 0.4 mmol) solved in methanol (5 mL) was added over a solution consisting in AzPy (0.04 g, 0.2 mmol) and methanol (5 mL). A small amount (10 drops) 2,6-dimethylpyridine was also added and the mixture was stirred for 3 h at room temperature when a solid phase was formed. This was removed by filtration and, in the clear filtrate, needle brown crystals grew in a few days. These were isolated, quicly cleaned with methanol, dried and characterised further. Yield: 0.064 g. The product proved to be soluble in THF, chloroform, hexane.

IR ν_{max} (KBr), cm^{-1}: 3435vw, 3086w, 3063w, 3034vw, 2924w, 2855w, 2781w, 2473m, 1859m, 1688s, 1593s, 1520w, 1474s, 1445s, 1408s, 1373s, 1352m, 1285vs, 1219s, 1159vs, 1105s, 1051s, 1022s, 1009vs, 916m, 872m, 837s, 822s, 785m, 737s, 598w, 569m, 550s, 525s, 507s, 488s, 473s, 432m, 382w.

UV-vis ($CHCl_3$), λ_{max} (ε)=287 nm (3316 $Lmol^{-1}cm^{-1}$), λ_{max}=460 (162 $Lmol^{-1}cm^{-1}$).

CONCLUSIONS

A supramolecular structure built up by co-crystallyzation of ferrocenecarboxylic acid with 4,4`-azopyridine in 2:1 molar ratio has been obtained and structurally characterized. The packing of the H-bonded associates in the crystal results into the formation of a three-dimensional supramolecular network mediated *via* C-H···π stacking interactions. The formation of hydrogen bonds between monocarboxyferrocene and 4,4'-azopyridine doesn't change the electron charge density around the nucleus ^{57}Fe, as Moessbauer spectra revealed. The cyclic voltammetry tehnique was used to evidence that the synthesized compund exhibits electrochemical behavior on both positive and negative potential range. The voltammograms show reversile and quasi-reversible anodic and cathodic peaks which can be subscribed to the oxidation and reduction of the ferrocene active center and to the azo group.

Acknowledgements: This work was supported by a grant of the Ministry of National Education, CNCS – UEFISCDI, Program PN-II-Capacities, Modul III, Roumania – Moldova Bilateral Cooperation (Project ComSilBio, Contract 690/16.04.2013).

REFERENCES

1. P. Du, J. Liu, G. Chen and M. Jiang, *Langmuir,* **2011**, *27*, 9602-9608, and references herein.
2. Q. Li, X. Chen, X. Yue, D. Huang and X. Wang, *Colloids Surf., A,* **2012**, *409*, 98-104, and references herein.
3. M. Munteanu, U. Kolb and H. Ritter, *Macromol. Rapid Commun.,* **2010**, *31*, 616-618, and references herein.
4. N. Sadhukhan, S.K. Patra, K. Sana and J.K. Bera, *Organometallics*, **2006**, *25*, 2914-2916.
5. C.M. Zakaria, G. Ferguson, A.J. Lough and C. Glidewell, *Acta Crystallogr., Sect. C: Cryst. Struct. Commun.,* **2003**, *59*, 271-274.
6. N. A. Wasio, R.C. Quardokus, R.P. Forrest, C.S. Lent, S.A. Corcelli, J.A. Christie, K.W. Henderson and S.A. Kandel, *Nature,* **2014**, *507*, 86-89.
7. C.B. Aakeroy, S. Panikkattu, B. DeHaven and J. Desper, *CrystEngComm*, **2013**, *15*, 463-470.
8. H. Liu, T. Kobayashi and T. Yu, *Macromol. Rapid Commun.,* **2011**, *32*, 378-383.
9. H. Han, A.H. Molla and P.K. Bhowmik, *Polym Prepr.* **1995**, *36*, 332-333.
10. G.K. Wertheim and R.H. Herber, *J.Chem.Phys.,* **1963**, *38*, 2106-2111.
11. I.P. Suzdalev, "Dynamic Effects in γ-Resonace Spectroscopy", Moscow: Atomizdat, 1979, 192, p. 9 (Russian language).
12. A. Vlad, M. Cazacu, C.Turta, I.R. Tigoianu, A. Airinei and A. Arvinte, *Synth. Met.* **2012**, *161,* 2659-2668.
13. CrysAlis RED, Oxford Diffraction Ltd.,Version 1.171.36.32, 2003.
14. O.V. Dolomanov, L.J. Bourhis, R.J. Gildea, J.A.K. Howard and H. Puschmann, *J. Appl. Cryst.,* **2009**, *42*, 339-341.
15. G.M. Sheldrick, *Acta Cryst. A,* **2008**, *64*, 112-122.